RSC Advances

PAPER

View Article Online
View Journal | View Issue

Cite this: *RSC Adv.*, 2020, **10**, 14331

N-Amino peptide scanning reveals inhibitors of $A\beta_{42}$ aggregation†

Khalilia C. Tillett [a] and Juan R. Del Valle *[b]

Received 2nd March 2020
Accepted 21st March 2020

DOI: 10.1039/d0ra02009e

rsc.li/rsc-advances

The aggregation of amyloids into toxic oligomers is believed to be a key pathogenic event in the onset of Alzheimer's disease. Peptidomimetic modulators capable of destabilizing the propagation of an extended network of β-sheet fibrils represent a potential intervention strategy. Modifications to amyloid-beta (Aβ) peptides derived from the core domain have afforded inhibitors capable of both antagonizing aggregation and reducing amyloid toxicity. Previous work from our laboratory has shown that peptide backbone amination stabilizes β-sheet-like conformations and precludes β-strand aggregation. Here, we report the synthesis of *N*-aminated hexapeptides capable of inhibiting the fibrillization of full-length $A\beta_{42}$. A key feature of our design is *N*-amino substituents at alternating backbone amides within the aggregation-prone $A\beta_{16-21}$ sequence. This strategy allows for maintenance of an intact hydrogen-bonding backbone edge as well as side chain moieties important for favorable hydrophobic interactions. An *N*-amino scan of $A\beta_{16-21}$ resulted in the identification of peptidomimetics that block $A\beta_{42}$ fibrilization in several biophysical assays.

Introduction

Amyloid protein aggregation has been linked to several neurodegenerative disorders, including Parkinson's and Alzheimer's Disease (AD).[1] In AD, amyloid precursor protein (APP) is sequentially cleaved by α and β secretase to release pathogenic amyloid beta (Aβ). Aβ is prone to aggregation and forms toxic β-sheet fibrils that are the main component of neuritic plaques in AD patients.[2] Of the two Aβ fragments formed during amyloidogenesis, the 42-residue variant ($A\beta_{42}$) is more prone to aggregation and displays greater neurotoxicity in comparison to the 40-residue variant ($A\beta_{40}$).[3] Soluble oligomers of $A\beta_{42}$ have been shown to impair hippocampal synaptic plasticity,[4] induce tau hyperphosphorylation,[5] activate microglial inflammation,[6] and impair memory.[7] Interestingly, studies have shown that high molecular weight oligomers are relatively inactive. However, when allowed to dissociate into low molecular weight oligomers (8–70 kDa) severe toxicity is observed. Additionally, soluble oligomers (but not monomers) cause synaptic death in a dose dependent manner.[8]

Although $A\beta_{42}$ is considered to be intrinsically disordered, its fibrils are comprised of parallel β-sheets that feature edge–edge hydrogen-bonding between $A\beta_{42}$ monomers.[9] This in-register association is driven in large part by a core hydrophobic sequence encompassing residues 16–21 ($_{16}$KLVFFA$_{21}$).[10] Direct $A\beta_{42}$ aggregation blockers that have entered clinical trials for the treatment of AD include homotaurine, scyllo-inositol, and sodium oligomannurarate.[11] These and similar compounds face significant hurdles to advancement, as they are likely to interact in a non-specific manner with β-rich target proteins. In contrast, backbone modified peptides derived from aggregation-prone segments offer the prospect of sequence-specific inhibition of amyloidogenesis. Toward this end, several groups have reported $A\beta_{16-21}$ peptidomimetics harboring D-amino acids, unnatural residues, or backbone amide substituents.[12] In addition to optimizing affinity for $A\beta_{42}$, such peptide modifications may serve to enhance proteolytic stability, conformational rigidity, and prospects for passage through the blood–brain barrier. Rationally designed peptidomimetics targeting $A\beta_{42}$ fibrilization have shown efficacy in animal models of AD.[12]

Our laboratory has previously shown that peptide backbone *N*-amination stabilizes β-sheet-like conformation through cooperative non-covalent interactions.[13] Like *N*-methylation, the incorporation of *N*-amino substituents within a peptide strand precludes canonical β-sheet associations along one of the hydrogen-bonding edges. This characteristic is useful for the design peptide derivatives that not only resist self-aggregation but also block β stacking of a target protein. Although backbone-methylated peptides are capable of disrupting Aβ aggregation,[14] we viewed *N*-amination as an alternative strategy for the design of more conformationally rigid β-breaker peptides. Unlike *N*-methylation or proline incorporation, backbone amination does not promote a significant population of the *cis* amide rotamer. Given that $A\beta_{42}$ fibrils adopt a β-strand

[a]*Department of Chemistry, University of South Florida, Tampa, Florida 33620, USA*
[b]*Department of Chemistry & Biochemistry, University of Notre Dame, Notre Dame, Indiana 46556, USA. E-mail: jdelvalle@nd.edu*

† Electronic supplementary information (ESI) available. See DOI: 10.1039/d0ra02009e

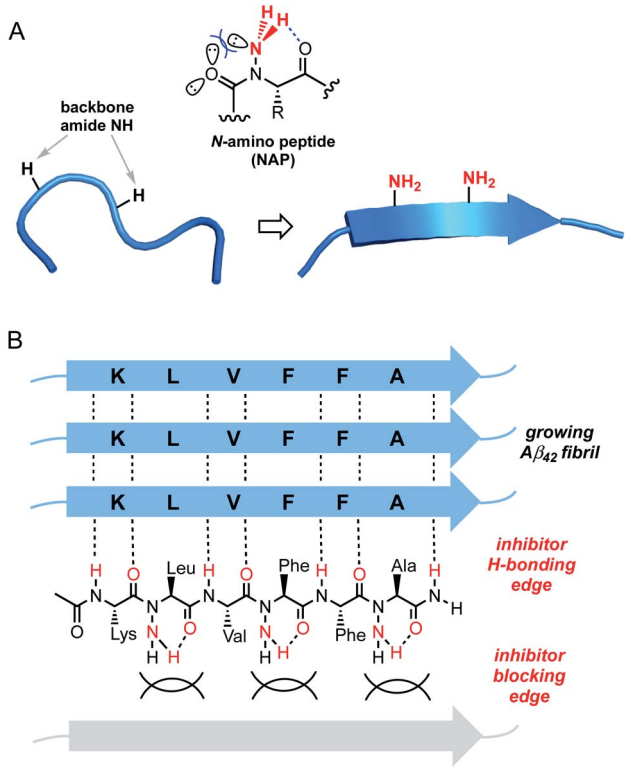

Fig. 1 Design of *N*-amino peptide (NAP) $A\beta_{16-21}$ mimics. (A) Conformational effects of peptide backbone *N*-amination. (B) Proposed model for inhibition of Aβ fibrilization by a representative NAP.

Table 1 Synthesis of α-hydrazino acid monomers for NAP scanning

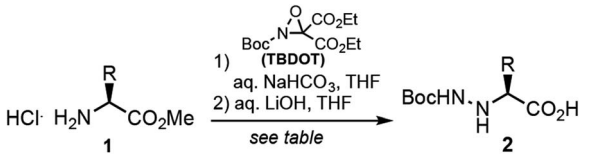

	Residue	R	Yield
2a	aLys(Boc)	$(CH_2)_4NHBoc$	74
2b	aLeu	$CH_2CH(CH_3)_2$	66
2c	aVal	$CH(CH_3)_2$	44
2d	aPhe	CH_2Ph	66
2e	aAla	CH_3	61

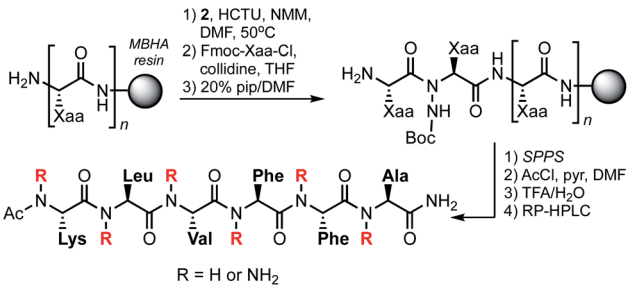

Scheme 1 Solid-phase synthesis of NAP-based $A\beta_{16-21}$ mimics.

conformation with an all-*trans* amide geometry, backbone-substituted mimics with high *trans* amide propensity should exhibit enhanced affinity for the conformationally extended core sequence. The *N*-amino group is also able to engage in an intraresidue C6 H-bond, which in turn stabilizes ψ and ϕ torsions in the β-sheet region of Ramachandran space.[13a] We sought to exploit these features in the design of β-strand peptidomimetics capable of blocking amyloid aggregation (Fig. 1). Here, we report the first example of *N*-amino peptide scanning and the identification of novel backbone-modified inhibitors of $A\beta_{42}$ fibrilization.

Results

Peptide *N*-amino scanning of the aggregation-prone $_{16}KLVFFA_{21}$ sequence required the synthesis of 5 distinct α-hydrazino acid derivatives starting from commercially available α-amino esters. We previously demonstrated that monomers suitable for solid-phase peptide synthesis (SPPS) can be readily accessed *via* electrophilic amination of α-amino esters.[15] As shown in Table 1, the requisite building blocks were thus prepared by treatment of **1** with (2-*t*-butyl-3,3-diethyl)-oxaziridine-2,3,3-tricarboxylate (TBDOT)[16] under aqueous conditions, followed by alkaline ester hydrolysis to give **2a–e** in good yields.

Backbone-aminated analogues of $A\beta_{16-21}$ were prepared on rink amide MHBA resin using Fmoc chemistry (Scheme 1). Condensation of the Boc-protected α-hydrazino acids onto the growing peptide chain was achieved by HCTU/NMM-mediated activation of the carboxylic acid in the presence of the unprotected Nα. The poorly nucleophilic Nα is only acylated upon exposure to pre-formed Fmoc-protected amino acid chloride derivatives.[17] These were prepared by reaction of Fmoc-protected amino acids with thionyl chloride, or by activation with Ghosez' reagent in the case of the Fmoc-Lys(Boc)-OH residue (due to the acid-labile side chain protecting group). Following sequence elongation, the peptidomimetics were *N*-terminally acetylated, cleaved from the resin, and purified by RP-HPLC.

Table 2 Synthesized $A\beta_{16-21}$ mimics and HRMS data

Peptide	Sequence	HRMS $[M + H]_{obs}^+$
3	Ac-Lys-Leu-Val-Phe-Phe-Ala-NH_2	779.4701
4	Ac-**aLys**-Leu-Val-Phe-Phe-Ala-NH_2	779.4697
5	Ac-Lys-**aLeu**-Val-Phe-Phe-Ala-NH_2	779.4714
6	Ac-Lys-Leu-**aVal**-Phe-Phe-Ala-NH_2	779.4711
7	Ac-Lys-Leu-Val-**aPhe**-Phe-Ala-NH_2	779.4680
8	Ac-Lys-Leu-Val-Phe-**aPhe**-Ala-NH_2	779.4687
9	Ac-Lys-Leu-Val-Phe-Phe-**aAla**-NH_2	779.4690
10	Ac-**aLys**-Leu-**aVal**-Phe-Phe-Ala-NH_2	794.4800
11	Ac-**aLys**-Leu-Val-Phe-**aPhe**-Ala-NH_2	794.4802
12	Ac-Lys-**aLeu**-Val-**aPhe**-Phe-Ala-NH_2	794.4811
13	Ac-Lys-**aLeu**-Val-Phe-Phe-**aAla**-NH_2	794.4802
14	Ac-Lys-Leu-**aVal**-Phe-**aPhe**-Ala-NH_2	794.4794
15	Ac-Lys-Leu-Val-**aPhe**-Phe-**aAla**-NH_2	794.4810
16	Ac-**aLys**-Leu-Val-Phe-Phe-Ala-NH_2	809.4920
17	Ac-Lys-**aLeu**-Val-**aPhe**-Phe-**aAla**-NH_2	809.4912

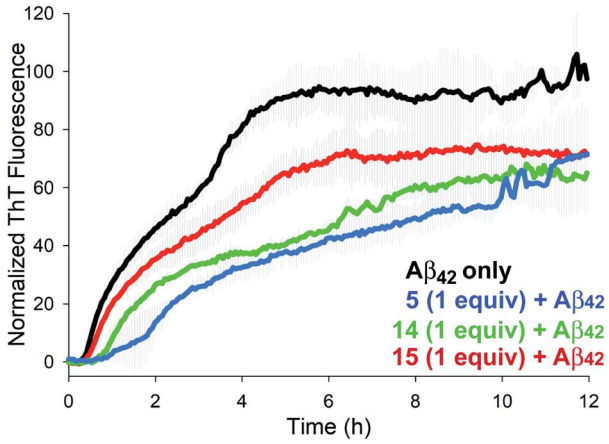

Fig. 2 Effects of 1.0 equiv. of inhibitors **5**, **14**, and **15** on $A\beta_{42}$ aggregation (40 μM) as monitored by ThT fluorescence.

For the current study, we synthesized the 14 *N*-aminated $A\beta_{16-21}$ variants shown in Table 2, along with the parent hexapeptide (**3**). This positional scanning library is comprised of all possible mono-aminated peptides, as well as di- and tri-aminated sequences that harbor backbone substituents on the same edge of the putative β-strand. We excluded analogues featuring alternate edge *N*-aminations since these compounds are presumably devoid of a fully intact hydrogen-bonding edge. The identity of purified peptidomimetics was confirmed by HRMS and their purities assessed by analytical HPLC and NMR. The ^{1}H NMR spectra for **3–17** were recorded in DMSO-d_6 and proton resonance assignments were made on the basis of TOCSY spectra.

The aggregation of $A\beta_{42}$ was monitored in the presence of 1 molar equivalent of NAPs **4–17** using thioflavin T (ThT), a dye that fluoresces upon binding to the perpendicular axis of amyloid fibrils (Fig. 2).[18] Compounds **5**, **14** and **15** were identified as the most effective inhibitors of $A\beta_{42}$ aggregation in repeated experiments. $A\beta_{42}$ fibrillization is typically characterized by a sigmoidal curve comprised of a lag phase, an elongation phase, and a plateau phase. Over a 12 h experiment, $A\beta_{42}$ aggregation was inhibited by approximately 30–50% at an equimolar ratio for each inhibitor. Although the peak fluorescence values of all three inhibitors were comparable, the elongation/growth phase of **5** and **14** were slower than that of **15**. In addition, **5** displayed increased lag times across all three runs (Fig. S1†). Although several other NAPs displayed some inhibitory effects on $A\beta_{42}$ aggregation kinetics, observed variations in repeated experiments led us to focus on compounds **5**, **14**, and **15** for further study. Consistent with previous reports, the parent hexapeptide **3** exhibited accelerated aggregation when incubated in the presence of $A\beta_{42}$ and ThT. Initial *in vitro* assay thus suggests that a single backbone amination, as in **5**, is sufficient to convert a highly aggregation-prone peptide into an inhibitor of fibrilization.

To gain further insight into the effects of NAPs **5**, **14**, and **15** on $A\beta_{42}$ structure we carried out circular dichroism (CD) measurements over several time points (Fig. 3). Incubation of

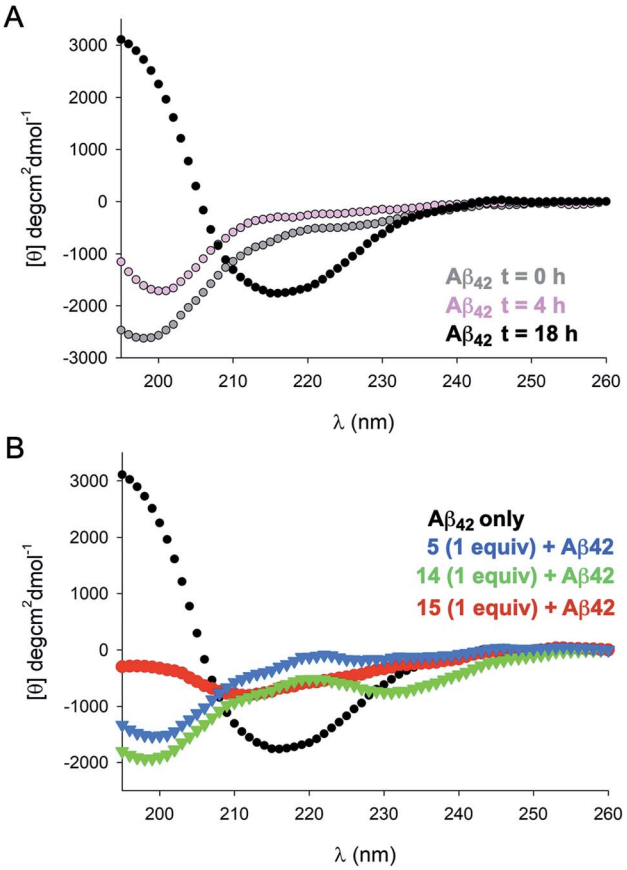

Fig. 3 Circular dichroism spectra. (A) Time-dependent CD spectra of 40 μM $A\beta_{42}$ recorded in phosphate buffer. (B) CD spectrum of $A\beta_{42}$ at 18 h (black), and in the presence of an equimolar ratio of **5**, **14**, and **15**.

$A\beta_{42}$ alone at 37 °C resulted in a transition from random coil to β-sheet structure over the course of 18 h, as evidenced by a pronounced minimum at 218 nm. Incubation of $A\beta_{42}$ in the presence of an equimolar concentration of **15** for 18 h resulted in a significantly attenuated β-sheet signature by CD, although some β-sheet character was still evident. In contrast, analogues **5** and **14** showed a similar CD signature at 18 h indicative of a random coil conformation. These spectra were also similar to those observed for $A\beta_{42}$ alone at 0 and 4 h timepoints. The Far UV-CD spectra of 40 μM **5**, **14**, and **15** revealed that each inhibitor showed irregular/random coil character in the absence of $A\beta_{42}$ (Fig. S2†).

Protofibrils, fibrillar precursors to amyloid formation, are preceded by the appearance of small Aβ oligomers.[19] Transmission electron microscopy (TEM) can be used to visualize the morphology of these fibril and pre-fibrillar species at high resolution. In order to assess the ability of **5**, **14**, and **15** to alter the dominant morphology of $A\beta_{42}$, samples were taken directly from the ThT assays at the plateau phase (Fig. 4). $A\beta_{42}$ incubated on its own formed a dense network of mature fibrils when incubated without inhibitor. $A\beta_{42}$ incubated with **5** showed scattered, short, rod-like protofibrils. No evidence of mature fibril formation was visible. $A\beta_{42}$ incubated with **14** showed little to no evidence of fibril formation, however, small seeding

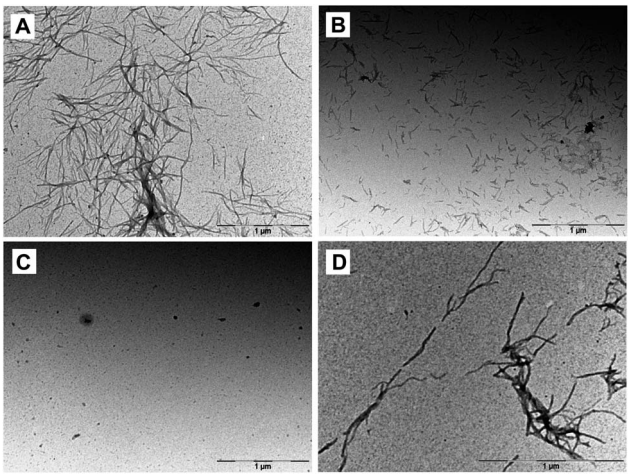

Fig. 4 Representative transmission electron microscopy images at t = 6 h. (A) $A\beta_{42}$ incubated alone, or in the presence of an equimolar amount of (B) **5**, (C) **14**, or (D) **15**.

was visible. $A\beta_{42}$ incubated with **15** showed sparse mature fibrils throughout the sample. These results are consistent with those from ThT assays and CD measurements showing that NAP **15** was not as effective as **5** or **14** in blocking the aggregation of $A\beta_{42}$ or its transition to β structure.

Based on results from TEM experiments, we investigated the ability of our most effective inhibitor to delay fibrilization in a dose-dependent manner by ThT. As shown in Fig. 5, **14** had little effect on aggregation lag time at 0.5 equiv. concentration, but delayed the aggregation of $A\beta_{42}$ by 80% and 220% at 1.0 equiv. and 4.0 equiv., respectively. Unlike **14**, we did not observe a similar dose-dependency in the case of **5** or **15**. Taken together, these data demonstrate that di-NAP **14** is effective in delaying $A\beta_{42}$ aggregation in a dose-dependent manner, inhibiting the formation of mature fibrils, and in blocking the transition of $A\beta_{42}$ from random coil to β structure *in vitro*.

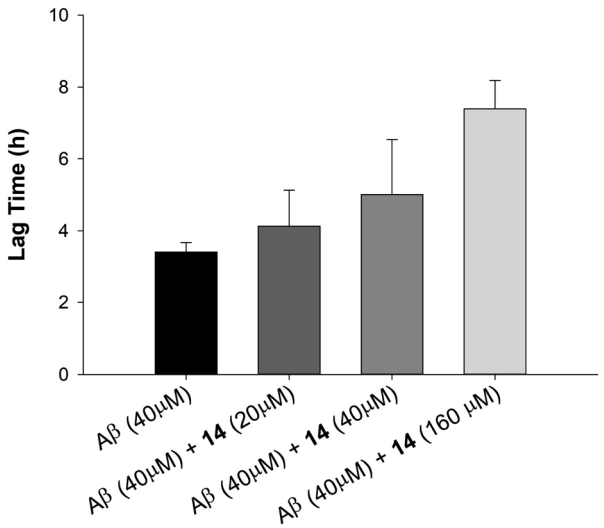

Fig. 5 Effect of 0.5, 1.0 and 4.0 equiv. of **14** on 40 μM $A\beta_{42}$ aggregation lagtime as monitored by ThT fluorescence assay.

Conclusions

Here, we demonstrate the synthesis and evaluation of *N*-amino peptide inhibitors of $A\beta_{42}$ aggregation that are readily accessible from α-hydrazino acid monomers. The inhibitory activity of selected NAPs was confirmed through ThT assay, CD, and TEM. Di-aminated derivative **14** emerged from this study as an effective inhibitor of $A\beta_{42}$ aggregation *in vitro*. Interestingly, tri-aminated derivatives **16** and **17** were less effective by ThT assay, as were the majority of mono-aminated analogues. We previously observed that di-amination across a tripeptide strand is a particularly powerful approach for stabilizing β-sheet conformations within hairpin model systems.[13] Peptidomimetics **14** and **15** likewise represent constrained β-strand mimics bearing two edge-blocking substituents in close proximity. This may explain their ability to engage $A\beta_{42}$ and shield one hydrogen-bonding edge from further association with Aβ monomers. The current work adds backbone *N*-amination to the repertoire of peptidomimetic strategies for targeting β-sheet assembly. We anticipate that this approach can be readily applied to other disease-relevant protein interactions and will provide useful lead compounds for structure-based refinement.

Experimental

Synthesis of compounds 3–17

Synthesis of all peptides/peptidomimetics was carried out on Fmoc-capped polystyrene rink amide MBHA resin (100–200 mesh). α-Hydrazino acid monomers were prepared from α-amino esters as previously described.[15] Dry resin was washed with DMF three times and allowed to swell in DMF for 1 h prior to use. All reactions were carried out using gentle agitation. Fmoc deprotection steps were carried out by treating the resin with a solution of 20%piperidine/DMF (15 min × 2). Coupling of Fmoc-protected amino acids as well as (*N*′-Boc)-hydrazino acids was effected using 5 equiv. HCTU (0.5 M in DMF), 10 equiv. NMM (1.0 M in DMF), and 5 equiv. of the carboxylic acid in DMF at 50 °C (1 h). Coupling of residues *N*-terminal to the hydrazino acids was carried out with 30 equiv. collidine and 10 equiv. of pre-formed Fmoc amino acid chloride[17] in THF at 45 °C (2 × 1 h). After each reaction the resin was washed with DMF three times. Peptides were cleaved from the resin by incubating with gentle stirring in 95 : 5 TFA : H_2O for 2 h. The cleavage mixture was filtered and the resin was rinsed with an additional portion of cleavage solution. The filtrate was concentrated to remove the bulk of the TFA and the remaining residue was treated with 8 mL of cold Et_2O to induce precipitation. The mixture was centrifuged and the supernatant was removed. The remaining solid was washed 2 more times with Et_2O and dried under vacuum. Peptides were analyzed and purified on C12 RP-HPLC columns (preparative: 4 μ, 90 Å, 250 × 21.2 mm; analytical: 4 μ, 90 Å, 150 × 4.6 mm) using linear gradients of MeCN/H_2O (with 0.1% formic acid), then lyophilized to afford white powders. All peptides were characterized by LCMS (ESI), HRMS (ESI-TOF), ^{1}H NMR, and TOCSY.

Thioflavin T fluorescence aggregation assay

ThT fluorescence assays were conducted in 96-well half area plates (black, flat bottom, non-binding surface) without shaking in a Biotek Synergy H1 microplate reader (444 nm excitation, 484 nm emission) at 37 °C for 12 h. Experiments were run in duplicate with 40 μM $A\beta_{42}$, 40 μM ThT, and 40 μM of inhibitor in 10 mM PBS buffer (pH 7.4) with a total reaction volume of 100 μL.

Composition of the wells of the 96-well plate. The ThT assay of $A\beta_{1-42}$ aggregation was performed by preparing stock solutions of 133.33 μM $A\beta_{42}$, 133.33 μM ThT, and 400 μM inhibitor and then adding 60, 30, and 10 μL portions, respectively, of these solutions into wells in a 96-well plate. $A\beta_{42}$ was added last. Prior to reading, the plate was incubated at 37 °C with orbital shaking for 3 min, then covered with an optically clear film.

Preparation of $A\beta_{42}$ stock solution. To disaggregate preformed $A\beta_{42}$ fibrils, lyophilized $A\beta_{42}$ was dissolved in HFIP and evaporated under vacuum to form a film. In order to delay further aggregation, the film was freshly dissolved in 10 mM aq. NaOH, followed by sonication for 30 s. This solution was further diluted into 10 mM PBS (pH 7.4) at a final concentration of 133.33 μM as a stock. This stock was then filtered through a pre-washed centricon filter (100 kD MW cutoff) at 6000 g, 4 °C for approximately 15 min.

Preparation of ThT stock solution. The ThT Stock solution was freshly prepared by dissolving 4 mg Thioflavin T powder in 20 mL 10 mM PBS (pH 7.4). This solution was filtered using a 13 mm syringe filter with 0.45 μM PTFE membrane. The concentration was determined by UV [$\varepsilon = 36\,000\ M^{-1}\ cm^{-1}$ at 412 nm] and diluted to final concentration using 10 mM PBS (pH 7.4).

Preparation of inhibitor stock solution. The inhibitor stock solutions were prepared by diluting a 20 mM DMSO stock first to 100× desired concentration using DMSO, and second to 10× desired concentration using 10 mM PBS (pH 7.4).

Circular dichroism. $A\beta_{42}$ was prepared as previously described,[20] and further diluted into 10 mM PBS (pH 7.4) to a final concentration of 80 μM. This stock solution was further diluted to 40 μM in Millipore water and incubated at 37 °C for 0 h, 4 h, and 18 h; incubation at 37 °C with shaking (0 h timepoint was recorded immediately after dilution). The spectra of $A\beta_{42}$ were recorded at 1.0 nm intervals from 195 to 260 nm with an averaging time of 3.0 s and an average of three repeats on an Aviv Stopped Flow CD spectropolarimeter (model 215). Inhibitor stock solutions of **5**, **14**, and **15** were prepared by dissolving the lyophilized powders into Millipore water at a final concentration of 80 μM. The spectra of each inhibitor were recorded using the method above. Additionally, the spectra of an equimolar solution of the $A\beta_{42}$ stock and each inhibitor stock were recorded after incubation for 18 h at 37 °C with shaking.

Transmission electron microscopy

Samples for TEM studies were taken from the ThT assay during the delayed lag phase. Each grid was prepared by aliquoting 10 μL of sample from the appropriate wells at the 6 h timepoint. The samples were pipetted onto formvar and carbon coated electron microscopy grids (Ted Pella, catalog no. 01754-F) and incubated for 3 min. Capillary action was used to remove the remaining liquid from the grids using filter paper. The grids were rinsed with Millipore water and stained with 1% (w/v) uranyl acetate solution. Samples were imaged using FEI M268D; Morgagni Series TEM.

Conflicts of interest

There are no conflicts to declare.

Acknowledgements

We thank Dr Kamlesh Makwana for assistance with data analysis and preparation of figures. This work was supported by a grant from the National Science Foundation (CHE1709927).

Notes and references

1 (*a*) F. Chiti and C. M. Dobson, Protein Misfolding, Functional Amyloid, and Human Disease, *Annu. Rev. Biochem.*, 2006, **75**, 333–366; (*b*) M. Bartolini and V. Andrisano, Strategies for the Inhibition of Protein Aggregation in Human Diseases, *ChemBioChem*, 2010, **11**, 1018–1035; (*c*) G.-f. Chen, T.-h. Xu, Y. Yan, Y.-r. Zhou, Y. Jiang, K. Melcher and H. E. Xu, Amyloid beta: structure, biology and structure-based therapeutic development, *Acta Pharmacol. Sin.*, 2017, **38**, 1205–1235; (*d*) D. J. Selkoe and J. Hardy, The amyloid hypothesis of Alzheimer's disease at 25 years, *EMBO Mol. Med.*, 2016, **8**, 595–608; (*e*) G. S. Bloom, Amyloid-β and Tau: The Trigger and Bullet in Alzheimer Disease Pathogenesis, *JAMA Neurology*, 2014, **71**, 505–508; (*f*) R. E. Tanzi and L. Bertram, Twenty Years of the Alzheimer's Disease Amyloid Hypothesis: A Genetic Perspective, *Cell*, 2005, **120**, 545–555.

2 A. E. Roher, J. D. Lowenson, S. Clarke, C. Wolkow, R. Wang, R. J. Cotter, I. M. Reardon, H. A. Zürcher-Neely, R. L. Heinrikson and M. J. Ball, Structural alterations in the peptide backbone of beta-amyloid core protein may account for its deposition and stability in Alzheimer's disease, *J. Biol. Chem.*, 1993, **268**, 3072–3083.

3 A. Lorenzo and B. A. Yankner, Beta-amyloid neurotoxicity requires fibril formation and is inhibited by congo red, *Proc. Natl. Acad. Sci. U. S. A.*, 1994, **91**, 12243–12247.

4 G. M. Shankar, S. Li, T. H. Mehta, A. Garcia-Munoz, N. E. Shepardson, I. Smith, F. M. Brett, M. A. Farrell, M. J. Rowan, C. A. Lemere, C. M. Regan, D. M. Walsh, B. L. Sabatini and D. J. Selkoe, Amyloid-beta protein dimers isolated directly from Alzheimer's brains impair synaptic plasticity and memory, *Nat. Med.*, 2008, **14**, 837–842.

5 Q. L. Ma, F. Yang, E. R. Rosario, O. J. Ubeda, W. Beech, D. J. Gant, P. P. Chen, B. Hudspeth, C. Chen, Y. Zhao, H. V. Vinters, S. A. Frautschy and G. M. Cole, Beta-amyloid oligomers induce phosphorylation of tau and inactivation of insulin receptor substrate via c-Jun N-terminal kinase

signaling: suppression by omega-3 fatty acids and curcumin, *J. Neurosci.*, 2009, **29**, 9078–9089.

6 S. Mandrekar-Colucci and G. E. Landreth, Microglia and inflammation in Alzheimer's disease, *CNS Neurol. Disord.: Drug Targets*, 2010, **9**, 156–167.

7 J. C. Dodart, K. R. Bales, K. S. Gannon, S. J. Greene, R. B. DeMattos, C. Mathis, C. A. DeLong, S. Wu, X. Wu, D. M. Holtzman and S. M. Paul, Immunization reverses memory deficits without reducing brain Abeta burden in Alzheimer's disease model, *Nat. Neurosci.*, 2002, **5**, 452–457.

8 T. Yang, S. Li, H. Xu, D. M. Walsh and D. J. Selkoe, Large Soluble Oligomers of Amyloid β-Protein from Alzheimer Brain Are Far Less Neuroactive Than the Smaller Oligomers to Which They Dissociate, *J. Neurosci.*, 2017, **37**, 152–163.

9 T. L. Benzinger, D. M. Gregory, T. S. Burkoth, H. Miller-Auer, D. G. Lynn, R. E. Botto and S. C. Meredith, Propagating structure of Alzheimer's beta-amyloid(10-35) is parallel beta-sheet with residues in exact register, *Proc. Natl. Acad. Sci. U. S. A.*, 1998, **95**, 13407–13412.

10 (*a*) C. Hilbich, B. Kisters-Woike, J. Reed, C. L. Masters and K. Beyreuther, Substitutions of hydrophobic amino acids reduce the amyloidogenicity of Alzheimer's disease βA4 peptides, *J. Mol. Biol.*, 1992, **228**, 460–473; (*b*) N. S. de Groot, F. X. Aviles, J. Vendrell and S. Ventura, Mutagenesis of the central hydrophobic cluster in Aβ42 Alzheimer's peptide, *FEBS J.*, 2006, **273**, 658–668.

11 F. Panza, M. Lozupone, G. Logroscino and B. P. Imbimbo, A critical appraisal of amyloid-β-targeting therapies for Alzheimer disease, *Nat. Rev. Neurol.*, 2019, **15**, 73–88.

12 D. Goyal, S. Shuaib, S. Mann and B. Goyal, Rationally Designed Peptides and Peptidomimetics as Inhibitors of Amyloid-β (Aβ) Aggregation: Potential Therapeutics of Alzheimer's Disease, *ACS Comb. Sci.*, 2017, **19**, 55–80.

13 (*a*) M. P. Sarnowski, C. W. Kang, Y. M. Elbatrawi, L. Wojtas and J. R. Del Valle, Peptide N-Amination Supports β-Sheet Conformations, *Angew. Chem., Int. Ed.*, 2017, **56**, 2083–2086; (*b*) M. P. Sarnowski, K. P. Pedretty, N. Giddings, H. L. Woodcock and J. R. Del Valle, Synthesis and beta-sheet propensity of constrained N-amino peptides, *Bioorg. Med. Chem.*, 2018, **26**, 1162–1166.

14 (*a*) N. Kokkoni, K. Stott, H. Amijee, J. M. Mason and A. J. Doig, N-Methylated peptide inhibitors of beta-amyloid aggregation and toxicity. Optimization of the inhibitor structure, *Biochemistry*, 2006, **45**, 9906–9918; (*b*) D. J. Gordon, R. Tappe and S. C. Meredith, Design and characterization of a membrane permeable N-methyl amino acid-containing peptide that inhibits Abeta1-40 fibrillogenesis, *J. Pept. Res.*, 2002, **60**, 37–55.

15 C. W. Kang, M. P. Sarnowski, Y. M. Elbatrawi and J. R. Del Valle, Access to Enantiopure α-Hydrazino Acids for N-Amino Peptide Synthesis, *J. Org. Chem.*, 2017, **82**, 1833–1841.

16 A. Armstrong, L. H. Jones, J. D. Knight and R. D. Kelsey, Oxaziridine-Mediated Amination of Primary Amines: Scope and Application to a One-Pot Pyrazole Synthesis, *Org. Lett.*, 2005, **7**, 713–716.

17 (*a*) L. A. Carpino, B. J. Cohen, K. E. Stephens, S. Y. Sadat-Aalaee, J. H. Tien and D. C. Langridge, (Fluoren-9-ylmethoxy)carbonyl (Fmoc) amino acid chlorides. Synthesis, characterization, and application to the rapid synthesis of short peptide segments, *J. Org. Chem.*, 1986, **51**, 3732–3734; (*b*) Y. M. Elbatrawi, C. W. Kang and J. R. Del Valle, Total Synthesis of L-156,373 and an oxoPiz Analogue via a Submonomer Approach, *Org. Lett.*, 2018, **20**, 2707–2710.

18 L. S. Wolfe, M. F. Calabrese, A. Nath, D. V. Blaho, A. D. Miranker and Y. Xiong, Protein-induced photophysical changes to the amyloid indicator dye thioflavin T, *Proc. Natl. Acad. Sci. U. S. A.*, 2010, **107**, 16863–16868.

19 L. C. Serpell, Alzheimer's amyloid fibrils: structure and assembly, *Biochim. Biophys. Acta*, 2000, **1502**, 16–30.

20 B. Bacsa, S. Bosze and C. O. Kappe, Direct solid-phase synthesis of the beta-amyloid (1-42) peptide using controlled microwave heating, *J. Org. Chem.*, 2010, **75**, 2103–2106.

